



Synthesis and Characterization of CuO Nanoparticles by the Chemical Liquid Deposition Method and Investigation of Its Catalytic Effect on the Thermal Decomposition of Ammonium Perchlorate

**Abbas Eslami,^{1*} Nafise Modanlou Juibari,¹
Seyed Ghorban Hosseini,² Maryam Abbasi¹**

¹ *Department of Inorganic Chemistry, Faculty of Chemistry,
University of Mazandaran, P.O. Box 47416-95447, Babolsar, Iran*

² *Department of Chemistry, Malek Ashtar University of Technology,
P.O. Box 16765-3454, Tehran, Iran*

**E-mail: Eslami@umz.ac.ir*

Abstract: Copper oxide nanoparticles have been synthesized by the chemical liquid deposition method and characterized by means of X-ray diffraction analysis (XRD), Fourier transform infrared spectroscopy (FT-IR) and scanning electron microscopy (SEM). The XRD and SEM results showed that the particle size was between 50 nm and 70 nm. Ammonium perchlorate (AP)-CuO nanostructures have been prepared by *ex-situ* mixing of AP and CuO nanoparticles, while AP/CuO nanocomposites have been obtained by *in-situ* growth of nano CuO on the surface of AP. The effect of the nanoparticles on the thermal decomposition of AP has been examined by differential scanning calorimetry (DSC) and thermogravimetric analysis (TGA) methods. The results showed that the *ex-situ* prepared nanoparticles had better catalytic activity than the *in-situ* prepared ones. The effect of the synthesized nanoparticles on the thermal decomposition of AP in experiments with a AP to CuO ratio of 98:2 was as follows: with the *ex-situ* prepared experiments, the decomposition temperature decreased from 428 °C to 348 °C and the heat released increased from 344 J·g⁻¹ to 1432 J·g⁻¹, while those with the *in-situ* prepared samples exhibited 341 °C and 1317 J·g⁻¹, respectively.

Keywords: copper oxide nanoparticles, *ex-situ* growth, ammonium perchlorate, thermal decomposition, chemical liquid deposition

1 Introduction

Nanoparticles of transition metal oxides (NTMO) have attracted a great deal of attention due to their unique applications in various fields, such as petrochemical, chemical, catalysts, photo-catalysts, solar cells and gas sensors, and their uses have increased remarkably since the mid-20th century [1, 2]. In recent years, many researchers have extensively investigated the catalytic activities of many nano transition metal oxides and associated composites. Ammonium perchlorate (AP) is known as the most common oxidizer in strategic military weapons and various solid propellants, and its efficiency in such applications is highly influenced by various transition metal oxides, especially when in a nano crystalline form [3]. The catalytic activity of these nano-metal oxide systems on the thermal decomposition of AP has usually been attributed to the higher surface area of the nanoparticles, the increase in defects in the nano-structures, and synergistic effects of the catalyst and support of the nano-composites [4-7].

Thermal decomposition of AP occurs through three well-known sequential processes [8] and the burning characteristic of AP-based propellants depends vitally on the decomposition characteristics of AP. This has been widely studied and attempts have been made to improve it by the use of various types of additives [9-13]. The DSC curve of pure AP shows one endothermic peak at around 241.2 °C and two exothermic peaks at 286 °C and 428 °C [14, 15]. The endothermic peak is due to the solid state phase transition from the orthorhombic to the cubic phase [14].

The most specific characteristic of the thermal decomposition of AP is that it occurs in two stages, namely, low temperature decomposition (at 286 °C), and high temperature decomposition (at 428 °C), commonly referred to as LTD and HTD, respectively [16]. Since a lower decomposition temperature causes a higher burning rate, catalysts that reduce the thermal decomposition temperature of AP are of great interest in the field of propellants [17, 18]. Some important parameters, such as the type, quantity, and particle size of the catalysts, as well as the mixing procedure of AP and the catalysts, are all crucial to the final decomposition temperature [19].

In fact, the catalytic thermal decomposition of AP and AP-based composite propellants is significantly susceptible to additives such as metal, metal powders, metal alloys and nano metal oxides. In this respect, different metal oxides such as CuO, ZnO, Fe₂O₃, Nd₂O₃, and Co₃O₄ with different sizes and morphologies have been studied for this purpose [5, 7, 20-22]. It has been shown that copper(II) oxide nanocrystals are a suitable additive for catalytic decomposition of AP, and can significantly reduce the HTD temperature and increase the heat released with

respect to pure AP [23]. This action of CuO can be considerably improved by decreasing its particle size to the nanometer scale [24].

Until now, several methods have been developed for the synthesis of NTMOs, which include microwave [25], hydrothermal [26], reverse microemulsion [27], melting [28] and the chemical liquid deposition method (CLD). Among these, the CLD method is a facile and cost effective route for synthesizing NTMOs that utilizes cheap, nontoxic and environmentally benign precursors [29]. The CLD method has promising advantages, such as a relatively low calcination temperature and produces homogenous and pure final materials [30-32].

In the present study, the CuO nanoparticles were synthesized by the chemical liquid deposition method at room temperature and mixed *ex-situ* with AP in different ratios. An important feature of the fabrication is the easy production process and the homogeneous precipitation of CuO nanoparticles. The CuO nanoparticles obtained exhibited excellent catalytic effects on the thermal decomposition of AP, in lowering the decomposition temperature and increasing the heat released. *In-situ* prepared samples, with similar CuO to AP ratios, have also been investigated for the catalytic effect of the CuO on the thermal decomposition of AP. The coating quality and thermal characteristics of the treated samples have been investigated by means of differential scanning calorimetry (DSC), X-ray diffraction (XRD) analysis, scanning electron microscopy (SEM), and Fourier transform infrared spectroscopy (FT-IR) spectroscopy.

2 Experimental

2.1 Materials and methods

$\text{Cu}(\text{NO}_3)_2 \cdot 3\text{H}_2\text{O}$, ethyl acetate ($\text{CH}_3\text{COOC}_2\text{H}_5$, 99.5%), and sodium hydroxide (NaOH) were purchased from Merck and AP (AR, d_{50} : 140 μm) (96%) was purchased from Fluka. The FT-IR spectra of the samples were recorded on an FT-IR spectrophotometer (BRUKER TENSOR 27) in the spectral range of 4000-400 cm^{-1} using KBr pellets. The crystal phase structures of the products were analyzed by X'Pert Pro MPD (PANalytical) X-ray using $\text{Cu K}\alpha$ radiation ($\lambda = 1.54 \text{ \AA}$) in the 2θ range from 20° to 70° . Scanning electron microscope (SEM) images were obtained by an EM-3200 operated at an accelerating voltage of 25 kV. Differential scanning calorimetry (DSC) measurements of finely powdered samples were performed using a Perkin-Elmer Pyris 6 DSC calorimeter at a heating rate of $10 \text{ }^\circ\text{C} \cdot \text{min}^{-1}$ in the temperature range 50-500 $^\circ\text{C}$ using alumina pans. Thermogravimetric (TGA) experiments were carried out using a Stanton

Redcroft, STA-780 series with aluminum crucibles, at a heating rate of $10\text{ }^{\circ}\text{C}\cdot\text{min}^{-1}$ in the temperature range $50\text{--}600\text{ }^{\circ}\text{C}$. The samples (about 3 mg) were placed in sealed aluminum pans under a nitrogen atmosphere at a flow rate of $20.0\text{ mL}\cdot\text{min}^{-1}$.

2.2 Preparative procedures

2.2.1 *Ex-situ synthesis*

For the synthesis of CuO nanoparticles, $\text{Cu}(\text{NO}_3)_2\cdot 3\text{H}_2\text{O}$ (0.12 g) was dissolved in ethyl acetate (60 mL) by vigorous stirring until completely dissolved. Subsequently, a desired volume of 0.5 M NaOH solution was added to the above solution, drop by drop, to produce precipitation. The product obtained was filtered off, washed several times with distilled water and dried for about 6 h at $80\text{ }^{\circ}\text{C}$ in an electric oven. The black CuO nanoparticle samples were characterized by FT-IR, XRD and SEM analyses. The CuO NP obtained (0.02 g) was added to AP (1 g) (for AP2) in an acetone medium, stirred for several minutes and then heated until solvent evaporation had occurred. The powders were dried in an electric oven at $80\text{ }^{\circ}\text{C}$ for 1 h. The conditions employed are summarized in Table 1.

Table 1. The synthetic conditions and catalytic properties of the prepared samples

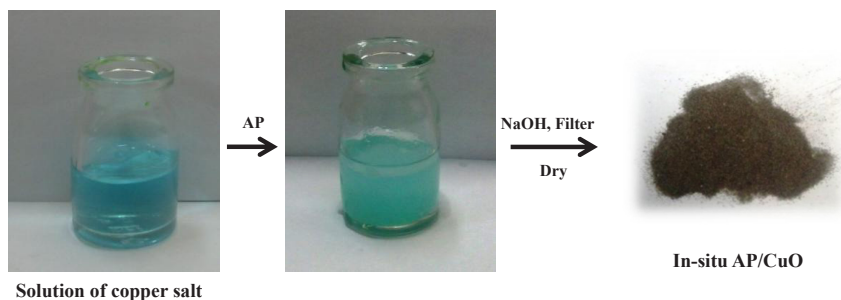
Sample	Metal salt	CuO [%]	Method	ΔT [$^{\circ}\text{C}$]	HTD [$^{\circ}\text{C}$]	ΔH [$\text{J}\cdot\text{g}^{-1}$]
AP0	-	-	-	181	428	344
AP1	$\text{Cu}(\text{NO}_3)_2\cdot 3\text{H}_2\text{O}$	2	<i>in-situ</i>	84	352	1317
AP2	$\text{Cu}(\text{NO}_3)_2\cdot 3\text{H}_2\text{O}$	2	<i>ex-situ</i>	92	348	1432
AP3	CuCl_2	4	<i>in-situ</i>	102	359	1072
AP4	$\text{Cu}(\text{NO}_3)_2\cdot 3\text{H}_2\text{O}$	4	<i>in-situ</i>	127	356	1009
AP5	$\text{Cu}(\text{NO}_3)_2\cdot 3\text{H}_2\text{O}$	4	<i>ex-situ</i>	90	342	1244
AP6	$\text{Cu}(\text{NO}_3)_2\cdot 3\text{H}_2\text{O}$	6	<i>in-situ</i>	116	355	817
AP7	$\text{Cu}(\text{NO}_3)_2\cdot 3\text{H}_2\text{O}$	6	<i>ex-situ</i>	84	338	928

ΔT is defined as the difference between the HTD and LTD values of the AP samples.

2.2.2 *In-situ synthesis*

In this synthetic procedure, the selected solvent should dissolve the metal salt but not the AP. For this purpose, ethyl acetate was chosen as the solvent. In the first step $\text{Cu}(\text{NO}_3)_2\cdot 3\text{H}_2\text{O}$ (0.02 g) (for AP1) was dissolved in ethyl acetate (30 mL) to produce the corresponding solution. Then, AP powder (1 g) was added to the solution as a template, followed by vigorous stirring to distribute the AP powder homogeneously in the solution. Subsequently, an appropriate volume of 0.5 M NaOH solution was added to the prepared mixture, drop by drop, to ensure the

metal ions in the solution had reacted with the NaOH and complete precipitation had taken place. The products were then filtered off and dried at 80 °C in an electric oven. A schematic representation of the details is shown in Scheme 1.



Scheme 1. Schematic representation of applied procedure

2.3 Catalytic activity test

The catalytic activity of the *in-situ* and *ex-situ* prepared nanocomposites were investigated through their performance in the thermal decomposition of AP. The details of these experiments are summarized in Table 1.

3 Results and Discussion

3.1 Crystalline structure (XRD)

The crystal structure of the CuO nanoparticles was characterized by X-ray diffraction (XRD) analysis. The XRD pattern of CuO nanoparticles is depicted in Figure 1. The XRD patterns show that all of the diffraction peaks are in good agreement with the standard diffraction data for CuO (JCPDS 45-0937), and no characteristic peaks were observed for other oxides (such as Cu₂O or Cu₂O₃).

Also, the average crystallite sizes (*D*) of the samples were calculated using the Debye-Scherrer Equation 1 from the major diffraction peaks [33]:

$$D = \frac{k\lambda}{\beta \cos\theta} \quad (1)$$

where *k* is a constant equal to 0.94, λ is the wavelength of Cu K α radiation, β is the full width at half maximum height (FWHM) of the diffraction peak in radians, and θ is the Bragg angles of the main planes. The average crystallite size estimated by applying the Debye-Scherrer equation was about 71 nm.

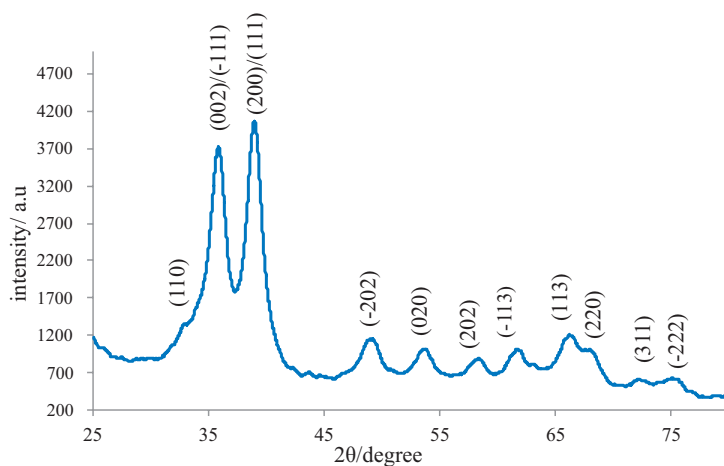


Figure 1. XRD pattern of copper oxide nanoparticles

3.2 Microscopic studies (SEM)

The surface morphology of the synthesized CuO nanoparticles was investigated using SEM analysis. The SEM images of the CuO NPs are shown in Figure 2. As may be seen, the mean particle size of CuO is about 50-70 nm and the nanoparticles have good homogeneity, spherical shape and appropriate separation. However, a few aggregates were also observed, which may be due to aggregation during the washing step. The particle size estimated from the SEM analysis is in good agreement with the XRD data. Such a small difference can be explained in terms of the global picture represented by XRD and the local features demonstrated by the SEM analysis.

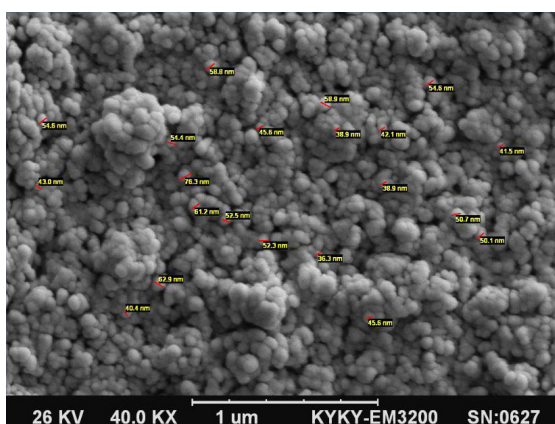


Figure 2. SEM image of copper oxide nanoparticles

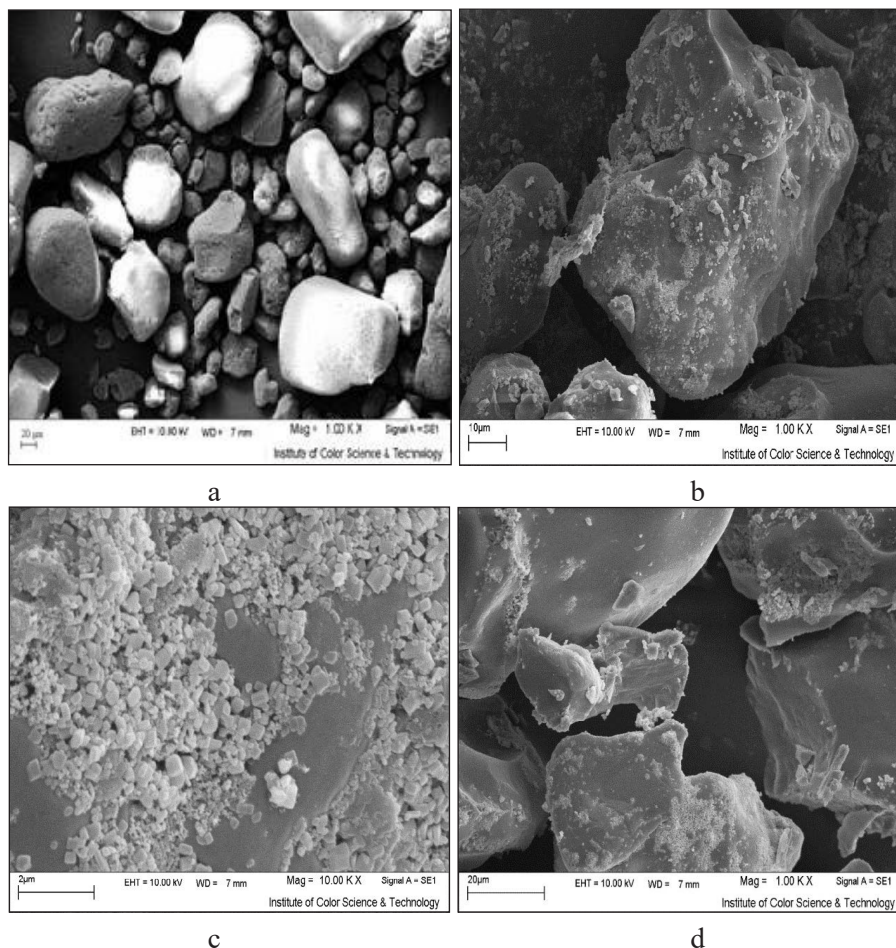


Figure 3. SEM image of AP0 (a), AP1 (b), CuO nanoparticles on the surface of AP (c), AP2 (d)

SEM images of pure AP (AP0) and the AP1 nanocomposite are shown in Figure 3. As may be seen in Figure 3a, the particles in pure AP varied between 20-80 μm, with smooth and clean surfaces. Compared with pure AP, the surfaces of the *in-situ* AP/CuO nanocomposites are evenly coated with nano CuO (Figure 3b) in which nanoparticles can be clearly observed on the surface of the AP (Figure 3c).

The SEM images of *ex-situ* AP-CuO nanocomposites are depicted in Figure 3d. It may be observed from these images that the appropriate precipitation had taken place and that the nanocomposite had been successfully synthesized.

3.3 FT-IR study

The vibrational properties of CuO NPs were studied by FT-IR spectroscopy and a spectrum is shown in Figure 4. As may be seen, the absorption bands at 3420 cm^{-1} and 1624 cm^{-1} can be ascribed to the OH stretching and HOH bending mode of adsorbed water, respectively [34], with three obvious absorption peaks around 588 cm^{-1} , 534 cm^{-1} and 435 cm^{-1} which can be assigned to the vibrations of the copper(II)–oxygen bonds [35]. There is also a tiny dip in the spectrum at 2363 cm^{-1} due to the presence of atmospheric CO_2 [36]. The FT-IR spectrum presented in Figure 4 is quite consistent with those of CuO in previous literature [37].

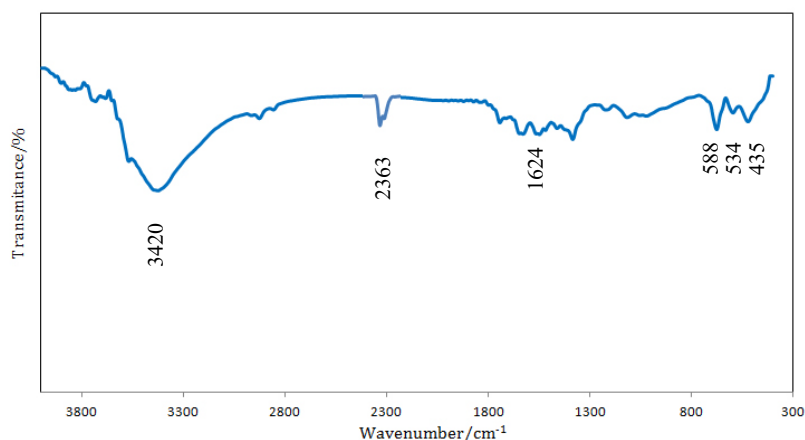
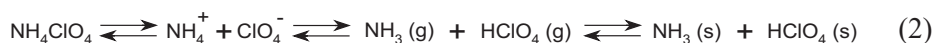


Figure 4. FT-IR spectrum of synthesized Copper oxide nanoparticles

3.4 Catalytic activity

The DSC curves of pure AP particles along with CuO treated AP (AP0-AP7) are shown in Figure 5 and the synthetic conditions and thermal properties of the samples are summarized in Table 1. The results show that the thermal decomposition of pure AP (AP0) occurs in two exothermic stages. The first stage, with an exothermic peak at $286\text{ }^{\circ}\text{C}$, is attributed to the partial decomposition of AP with an initial mass loss of about 30%. In this stage some gaseous intermediates, such as NH_3 and HClO_4 , are formed through partial dissociation and sublimation [38, 39], as follows:



Since the reaction between the evolved HClO_4 and NH_3 is incomplete at

low temperatures, some of these species are adsorbed onto the solid surface of unreacted AP. The first stage of decomposition of AP stops when the surface of AP is totally covered by adsorbed HClO_4 and NH_3 .

As the temperature increases to about $380\text{ }^\circ\text{C}$, the second stage of decomposition of AP commences in which reactions between the adsorbed HClO_4 , NH_3 and other species lead to complete decomposition of AP and the production of several final volatile molecules, such as HCl , H_2O , N_2O , Cl_2 , NO , O_2 , and NO_2 . This stage is known as the HTD of ammonium perchlorate and is accompanied with a mass loss of about 70% [40-42].

The catalytic effect of *ex-situ* synthesized CuO and *in-situ* grown CuO nanoparticles on the surface of AP in the thermal decomposition of AP was investigated by DSC analysis. The *ex-situ* AP/CuO nanocomposites with ratios of 98:2, 96:4 and 94:6 (AP2, AP5 and AP7) show significant reductions of the high decomposition temperature (HTD) from $428\text{ }^\circ\text{C}$ for AP0 to about $348\text{ }^\circ\text{C}$, $342\text{ }^\circ\text{C}$, and $338\text{ }^\circ\text{C}$ respectively, and for *in-situ* nanocomposites AP1, AP4 and AP6, the HTD is reduced to $341\text{ }^\circ\text{C}$, $356\text{ }^\circ\text{C}$ and $355\text{ }^\circ\text{C}$, respectively. Furthermore, a pronounced increase in the heat evolved occurs upon treatment of the AP particles as *ex-situ* and *in-situ* nanocomposites, being greater with *ex-situ* nanocomposites, and the best result occurring with AP2 with a 98:2 ratio in the *ex-situ* nanocomposite, the heat released being $1432\text{ J}\cdot\text{g}^{-1}$. The effect of the chloride salt of copper, as an alternative to the nitrate salt, was examined at a ratio of 96:4 (AP3). These results showed that the nitrate salt was a better precursor, and thus was employed in further experiments. There have been many studies on the mechanism of the effect of nanoparticles as catalysts in the thermal decomposition of AP, but this still remains unresolved [24]. However, from these studies two mechanisms were proposed which are based on the proton and electron transfer theory and are associated with the LTD and HTD, respectively [38]. According to the proton transfer theory, decomposition starts through proton transfer from NH_4^+ to ClO_4^- (Equation 2) and then further reactions cause partial decomposition of AP. From the electron transfer theory, the main decomposition stage, which occurs at higher temperatures, is initiated by electron transfer from anion to cation which leads to NH_4^0 and ClO_4^0 species [43]:



It is believed that this electron transfer reaction is a key step in the thermal decomposition of AP, which significantly affects the rate and types of relevant reactions. It is also greatly influenced by the presence of electron mediators which can facilitate electron transfer from ClO_4^- to NH_4^+ . In this view, the

catalytic activity of CuO can be attributed to the active d shell of $\text{Cu}^{2+}(3d^9)$ in CuO which can be changed into the stable fully-filled 3d-orbital form of $\text{Cu}^+(3d^{10})$ and the electron transfer can be accelerated as result of concurrent contact of the copper atom with NH_4^+ and ClO_4^- according to following equations [44-46] (Equations 4, 5):



The ammonium radical could then decompose to ammonia and a hydrogen atom:



Atomic H and ClO_4^0 interact with each other and produce HClO_4 , which can interact further with H as represented in the following equation:



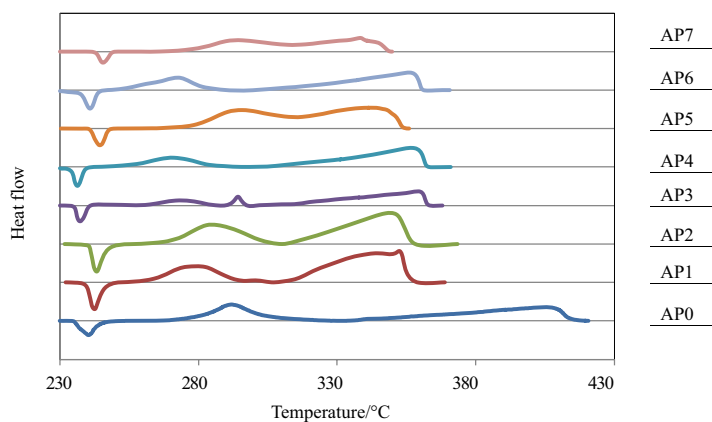
The ClO_3 radical can act as an electron scavenger and become converted to ClO_3^- which can react with NH_3 in the gas phase resulting in various species such as O_2 , N_2O , Cl_2 , NO and H_2O [8].

Ammonia formation in the presence of metal oxide nanoparticles can also be discussed based on proton transfer theory [36], in which reaction of NH_4^+ with surface oxide ions of spinel accelerates NH_3 formation (Equation 8) and subsequent reactions.

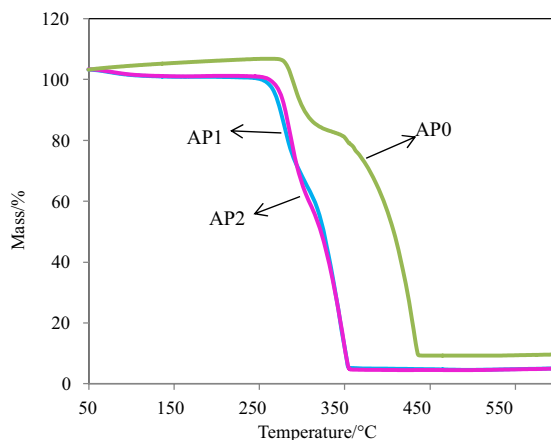


The oxide ions, together with other products of the decomposition of HClO_4 , could then oxidize NH_3 and complete the decomposition of AP [19].

On the other hand, heat release or energy release is one of the most important properties of the thermal decomposition and combustion of AP and AP-based solid composite propellants. Catalysts always play a key role in the heat releasing processes of propellants. Due to the higher surface to volume ratio of nano particles, nano-catalysts are likely to exhibit much higher catalytic efficiency than micro catalysts [47].



a

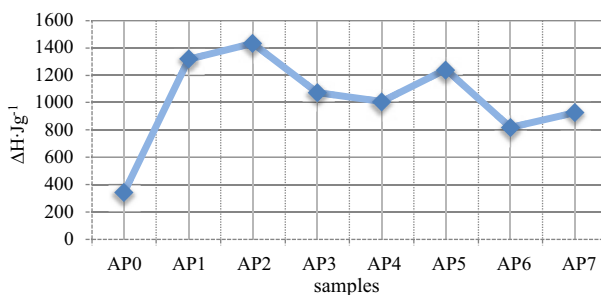


b

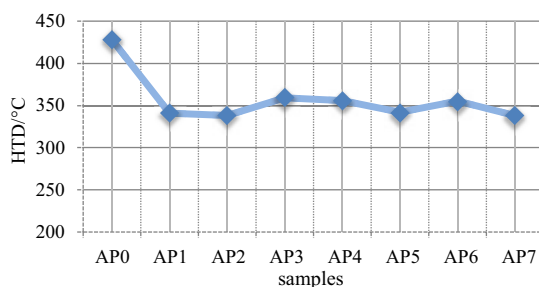
Figure 5. DSC and TGA curve of AP0-AP7 (a), and TGA curve of AP0, AP1 and AP2 at heating rate of $10^{\circ}\text{C}\cdot\text{min}^{-1}$ sample mass 3 mg; N_2 atmosphere

Although many investigations have been carried out on the catalytic improvement of the thermal decomposition properties of AP particles by different nano-additives and two major mechanisms, involving electron transfer from perchlorate ion to ammonium ion and proton transfer from ammonium ion to perchlorate ion, have been proposed for the thermal decomposition of AP [20-22], the mechanistic studies on the effect of nano-additives on thermal decomposition of AP have rarely been performed [48]. However that may be explained by two proposed approaches. Firstly, the higher surface area of nano relative to

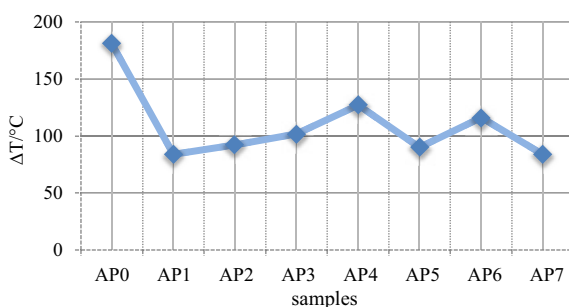
micro particles results in less sputtering of the particles during decomposition. This causes less mechanical loss and more efficient heat transfer within the nanocomposite, causing high heat release. Another reason for the higher heat release may be attributed to the efficient combustion of NH_3 with chlorine oxides in the presence of CuO nanoparticles involved in Equations 3-8 [48, 49].



a



b



c

Figure 6. Variation of decomposition released heat (a), HTD temperature (b) and difference between HTD and LTD (c) for pure AP (AP0) and treated samples

The TGA curves of AP0 along with AP1 and AP2, which are the best catalyzed samples, are shown in Figure 5b. It may be observed that the thermal decomposition of the catalyzed samples occurs at a lower and narrower temperature range, especially in the second step. So, we can attribute any improvement in the thermal decomposition of AP mainly to the action of copper oxides nanoparticles.

The variations in the thermal decomposition properties of pure AP and the treated samples are shown in Figure 6. As may be seen in Figure 6a, the heat of decomposition of AP2 is higher than those of the others, and, according to Figure 6b, the decomposition temperature for AP1 is lower than that of the other samples. The differences between HTD and LTD are shown in Figure 6c.

In order to obtain a better view of the catalytic activity of the prepared CuO nanoparticles, the results of this study were compared with literature reports. As shown in Table 2, the prepared CuO nanoparticles exhibited good catalytic activity in decreasing the HTD temperature and increasing the heat released from AP compared to previously reported copper oxide nanoparticles.

Table 2. Catalytic activity of the different synthesized CuO nanoparticles on the thermal decomposition of treated ammonium perchlorate particles

No.	AP/Metal ratio	Method of synthesis*	HTD [°C]	Reference
1	100:0	-	428	This work
2	100:2	Electrochemical	360	[23]
3	100:3	Sol-gel	353	[43]
4	100:1	Commercial	359	[50]
5	100:2	Commercial	348	[50]
6	100:3	Commercial	347	[50]
7	100:2	Deposition	364	[51]
8	100:2	CLD (<i>ex-situ</i>)	348	This work
9	100:2	CLD (<i>in-situ</i>)	341	This work

* CLD: chemical liquid deposition method

In summary, based on the experimental results that are represented in Figures 5 and 6 and Table 1, the *ex-situ* prepared CuO nanoparticles, have a slightly better catalytic effect on the thermal decomposition of ammonium perchlorate than the *in-situ* prepared ones.

4 Conclusions

Ex-situ and *in-situ* AP-CuO nanocomposites were successfully synthesized by a facile chemical liquid deposition method at room temperature and evaluated for their catalytic properties on the thermal decomposition of AP. The results showed that *ex-situ* nanocomposites have a better effect on the thermal decomposition of AP. SEM images showed that the synthesized CuO NPs were uniformly coated on the surface of AP in the *in-situ* experiments. It was found that both *in-situ* and *ex-situ* AP-CuO nanocomposites have good catalytic activity in lowering the thermal decomposition temperature and increasing the heat released and that the *ex-situ* samples have a slightly better catalytic effect than the *in-situ* ones. The DSC results indicated that the *ex-situ* AP/CuO nanocomposite (AP2), which has a 98:2 AP to metal weight ratio, exhibits the highest catalytic activity.

Acknowledgement

We gratefully acknowledge financial support from the Research Council of the University of Mazandaran.

References

- [1] Fierro, J. L. G. *Metal Oxides Chemistry and Applications*. Taylor & Francis, Boca Raton, **2006**; ISBN 9780824723712.
- [2] Tiwari, A.; Mishra, A. K.; Kobayashi, H.; Turner, A. P. (Eds.), *Intelligent Nanomaterials: Processes, Properties, and Applications*. John Wiley & Sons Scrivener Pub., Hoboken, **2012**; ISBN 9780470938799.
- [3] Cain, J.; Brewster, M.Q. Radiative Ignition of Fine-Ammonium Perchlorate Composite Propellants. *Propellants Explos. Pyrotech.* **2006**, *31*(4): 278-284.
- [4] Li, L.; Sun, X.; Qiu, X.; Xu, J.; Li, G. Nature of Catalytic Activities of CoO Nanocrystals in Thermal Decomposition of Ammonium Perchlorate. *Inorg. Chem.* **2008**, *47*(19): 8839-8846.
- [5] Yin, J.; Lu, Q.; Yu, Z.; Wang, J.; Pang, H.; Gao, F. Hierarchical ZnO Nanorod-assembled Hollow Superstructures for Catalytic and Photoluminescence applications. *Cryst. Growth Des.* **2009**, *10*(1): 40-43.
- [6] Sun, X.; Qiu, X.; Li, L.; Li, G. ZnO Twin-cones: Synthesis, Photoluminescence, and Catalytic Decomposition of Ammonium Perchlorate. *Inorg. Chem.* **2008**, *47*(10): 4146-4152.
- [7] Zhu, J.; Zeng, G.; Nie, F.; Xu, X.; Chen, S.; Han, Q.; Wang, X. Decorating Graphene Oxide with CuO Nanoparticles in a Water-Isopropanol System. *Nanoscale* **2010**, *2*(6): 988-994.
- [8] Eslami, A.; Hosseini, S. G.; Bazrgary, M. Improvement of Thermal Decomposition

- Properties of Ammonium Perchlorate Particles Using Some Polymer Coating Agents. *J. Therm. Anal. Calorim.* **2013**, *113*(2): 721-730.
- [9] Ma, Z.; Li, F. Preparation and Thermal Decomposition Behavior of TMOS/AP Composite Nanoparticles. *Nanoscience* **2006**, *11*: 142-145.
- [10] Yuan, Y.; Jiang, W.; Wang, Y.; Shen, P.; Li, F.; Li, P.; Zhao, F.; Gao, H. Hydrothermal Preparation of Fe₂O₃/Graphene Nanocomposite and its Enhanced Catalytic Activity on the Thermal Decomposition of Ammonium Perchlorate. *Appl. Surf. Sci.* **2014**, *303*: 354-359.
- [11] Zhang, Z. K.; Guo, D. Z.; Zhang, G. M. Preparation, Characterization and Catalytic Property of CuO Nano/Microspheres via Thermal Decomposition of Cathode-plasma Generating Cu₂(OH)₃NO₃ Nano/Microspheres. *J. Colloid Interface Sci.* **2011**, *357*(1): 95-100.
- [12] Li, Z.; Xiang, X.; Bai, L.; Li, F. A Nanocomposite Precursor Strategy to Mixed-metal Oxides with Excellent Catalytic Activity for Thermal Decomposition of Ammonium Perchlorate. *Appl. Clay Sci.* **2012**, *65*: 14-20.
- [13] Luo, Y. X.; Lu, L. D.; Liu, X. H.; Yang, X. J.; Wang, X. Synthesis of Nanocrystalline CuO and its Catalytic Activity on the Thermal Decomposition of NH₄ClO₄. *Chin. J. Inorg. Chem.* **2002**, *18*(12): 1211-1214.
- [14] Cheng, Z. P.; Xu, J. M.; Zhong, H.; Chu, X. Z.; Song, J. Novel Urchin-like Pd Nanostructures Prepared by a Simple Replacement Reaction and their Catalytic Properties. *Appl. Surf. Sci.* **2011**, *257*(18): 8028-8032.
- [15] Vyazovkin, S.; Wight, C. A. Kinetics of Thermal Decomposition of Cubic Ammonium Perchlorate. *Chem. Mater.* **1999**, *11*(11): 3386-3393.
- [16] Solymosi, F.; Krix, E. Catalysis of Solid Phase Reactions Effect of Doping of Cupric Oxide Catalyst on the Thermal Decomposition and Explosion of Ammonium Perchlorate. *J. Catal.* **1962**, *1*(5): 468-480.
- [17] Jacobs, P. W. M.; Whitehead, H. M. Decomposition and Combustion of Ammonium Perchlorate. *Chem. Rev.* **1969**, *69*(4): 551-590.
- [18] Jain, S. R.; Nambiar, P. R. Effect of Tetramethylammonium Perchlorate on Ammonium Perchlorate and Propellant Decomposition. *Thermochim. Acta* **1976**, *16*(1): 49-54.
- [19] Li, N.; Geng, Z.; Cao, M.; Ren, L.; Zhao, X.; Liu, B.; Tian, Y.; Hu, C. Well-dispersed Ultrafine Mn₃O₄ Nanoparticles on Graphene as a Promising Catalyst for the Thermal Decomposition of Ammonium Perchlorate. *Carbon* **2013**, *54*: 124-132.
- [20] Charavarthy, S. R.; Price, E. W.; Sigman, R. K. Mechanism of Burning Rate Enhancement of Composite Solid Propellants by Ferric Oxide. *J. Prop. Power* **1997**, *13*(4): 471-480.
- [21] Survase, D. V.; Gupta, M.; Asthana, S. N. The Effect of Nd₂O₃ on Thermal and Ballistic Properties of Ammonium Perchlorate (AP) Based Composite Propellants. *Prog. Cryst. Growth. Charact. Mater.* **2002**, *45*(1): 161-165.
- [22] Zhou, H.; Lv, B.; Wu, D.; Xu, Y. Synthesis of Polycrystalline Co₃O₄ Nanowires with Excellent Ammonium Perchlorate Catalytic Decomposition Property. *Mater.*

- Res. Bull.* **2014**, *60*: 492-497.
- [23] Patil, P. R.; Krishnamurthy, V. E.; Joshi, S. S. Effect of Nano-copper Oxide and Copper Chromite on the Thermal Decomposition of Ammonium Perchlorate. *Propellants Explos. Pyrotech.* **2008**, *33*(4): 266-270.
- [24] Chaturvedi, S.; Dave, P. N. Nano-metal Oxide: Potential Catalyst on Thermal Decomposition of Ammonium Perchlorate. *J. Exp. Nanosci.* **2012**, *7*(2): 205-231.
- [25] Karunakaran, C.; Rajeswari, V.; Gomathisankar, P. Optical, Electrical, Photocatalytic, and Bactericidal Properties of Microwave Synthesized Nanocrystalline Ag-ZnO and ZnO. *Solid State Sci.* **2011**, *13*(5): 923-928.
- [26] Chen, L.; Zhu, D. The Particle Dimension Controlling Synthesis of α -MnO₂ Nanowires with Enhanced Catalytic Activity on the Thermal Decomposition of Ammonium Perchlorate. *Solid State Sci.* **2014**, *27*: 69-72.
- [27] Abazari, R.; Sanati, S.; Perovskite, L. FeO₃ Nanoparticles Synthesized by the Reverse Microemulsion Nanoreactors in the Presence of Aerosol-OT: Morphology, Crystal Structure, and their Optical Properties. *Superlattices Microstruct.* **2013**, *64*: 148-157.
- [28] Al-Syadi, A. M.; Yousef, E. S.; El-Desoky, M. M.; Al-Assiri, M. S. Kinetic Characterization of Barium Titanate-Bismuth Oxide-Vanadium Pentoxide Glasses. *Solid State Sci.* **2014**, *32*: 48-55.
- [29] Weber, R. W.; Moller, K. P.; O'Connor, C. T. The Chemical Vapour and Liquid Deposition of Tetraethoxysilane on ZSM-5, Mordenite and Beta. *Microporous Mesoporous Mater.* **2000**, *35*: 533-543.
- [30] Zhou, J. G.; Addison, A.; He, Z.; Wang, F. Chemical Liquid Deposition Process for Microstructure Fabrication. *Mater. Des.* **2005**, *26*(8): 670-679.
- [31] Yue, Y. H.; Tang, Y.; Liu, Y.; Gao, Z. Chemical Liquid Deposition Zeolites with Controlled Pore-opening Size and Shape-selective Separation of Isomers. *Ind. Eng. Chem. Res.* **1996**, *35*(2): 430-433.
- [32] Zhang, B.; Wang, C.; Lang, L.; Cui, R.; Liu, X. Selective Defect-patching of Zeolite Membranes Using Chemical Liquid Deposition at Organic/Aqueous Interfaces. *Adv. Funct. Mater.* **2008**, *18*(21): 3434-3443.
- [33] Cullity, B. D.; Stock, S. R. *Elements of X-ray Diffraction*. Pearson Education, Harlow, **2014**; ISBN 9781292040547.
- [34] Sugama, T. Yttrium Acetate-derived Particle Coatings for Mitigating Oxidation and Corrosion of Inconel 625. *J. Sol-Gel Sci. Technol.* **1998**, *12*(1): 35-48.
- [35] Chen, L.; Li, L.; Li, G. Synthesis of CuO Nanorods and their Catalytic Activity in the Thermal Decomposition of Ammonium Perchlorate. *J. Alloy. Compd.* **2008**, *464*(1): 532-536.
- [36] Darezereshki, E. Synthesis of Maghemite (γ -Fe₂O₃) Nanoparticles by Wet Chemical Method at Room Temperature. *Mater. Lett.* **2010**, *64*(13): 1471-1472.
- [37] Chen, L. J.; Li, L. P.; Li, G. S. Synthesis of CuO Nanorods and their Catalytic Activity in the Thermal Decomposition of Ammonium Perchlorate. *J. Alloys Compd.* **2008**, *464* (1): 532-536.
- [38] Boldyrev, V. Thermal Decomposition of Ammonium Perchlorate. *Thermochim.*

- Acta* **2006**, *443*(1): 1-36.
- [39] Li, L.; Zhou, Y.; Li, Z.; Ma, Y.; Pei, C. One Step Fabrication of Mn_3O_4 /Carbonated Bacterial Cellulose with Excellent Catalytic Performance upon Ammonium Perchlorate Decomposition. *Mater. Res. Bull.* **2014**, *60*: 802-807.
- [40] Jacobs, P. W. M.; Pearson, G. S. Mechanism of the Decomposition of Ammonium Perchlorate. *Combust. Flame* **1969**, *13*(4): 419-430.
- [41] Rosser, W. A.; Inami, S. H.; Wise, H. Thermal Decomposition of Ammonium Perchlorate. *Combust. Flame* **1968**, *12*(5): 427-435.
- [42] Devi, T. G.; Kannan, M. P.; Hema, B. Thermal Decomposition of Cubic Ammonium Perchlorate – the Effect of Barium Doping. *Thermochim. Acta* **1996**, *285*(2): 269-276.
- [43] Alizadeh-Gheshlaghi, E.; Shaabani, B.; Khodayari, A.; Azizian-Kalandaragh, Y.; Rahimi, R. Investigation of the Catalytic Activity of Nano-sized CuO , Co_3O_4 and $CuCo_2O_4$ Powders on Thermal Decomposition of Ammonium Perchlorate. *Powder Technol.* **2012**, *217*: 330-339.
- [44] Chaturvedi, S.; Dave, P. N. A Review on the Use of Nanometals as Catalysts for the Thermal Decomposition of Ammonium Perchlorate. *J. Saudi Chem. Soc.* **2013**, *17*(2): 135-149.
- [45] Hosseini, S. G.; Abazari, R. A Facile One-step Route for Production of CuO , NiO , and CuO - NiO Nanoparticles and Comparison of their Catalytic Activity for Ammonium Perchlorate Decomposition. *RSC Adv.* **2015**, *117*: 96777-96784.
- [46] Eslami, A.; Juibari, N. M.; Hosseini, S. G. Fabrication of Ammonium Perchlorate/Copper-Chromium Oxides Core-shell Nanocomposites for Catalytic Thermal Decomposition of Ammonium Perchlorate. *Mater. Chem. Phys.* **2016**, *181*: 12-20.
- [47] Yang, Y.; Yu, X.; Wang, J.; Wang, Y. Effect of the Dispersibility of Nano- CuO Catalyst on Heat Releasing of AP/HTPB Propellant. *J. Nanomater.* **2011**, Article ID 180896.
- [48] Patil, P. R.; Krishnamurthy, V. N.; Joshi, S. S. Differential Scanning Calorimetric Study of HTPB Based Composite Propellants in Presence of Nano Ferric Oxide. *Propellants Explos. Pyrotech.* **2006**, *31*(6): 442-446.
- [49] Joshi, S. S.; Patil, P. R.; Krishnamurthy, V. N. Thermal Decomposition of Ammonium Perchlorate in the Presence of Nanosized Ferric Oxide. *Def. Sci. J.* **2008**, *58*(6): 271-272.
- [50] Mahinroosta, M. Catalytic Effect of Commercial Nano- CuO and Nano- Fe_2O_3 on Thermal Decomposition of Ammonium Perchlorate. *J. Nanostructure Chem.* **2013**, *3*(1): 1-6.
- [51] Wang, J.; He, S.; Li, Z.; Jing, X.; Zhang, M.; Jiang, Z. Synthesis of Chrysalis-like CuO Nanocrystals and their Catalytic Activity in the Thermal Decomposition of Ammonium Perchlorate. *J. Chem. Sci.* **2009**, *121*(6): 1077-1081.